is a stronger reducing agent by about 0.1 V, also suggests a significant reorganizational component to the rate advantage for adduct formation with these copper complexes. This would be plausible in view of the observations on simpler electron-transfer reactions, but there is at present no way to assess the contribution to ΔG_{ab}^{*} that originates from the stability of the Cu^{II}–(O_2^{2-}) bond, a factor which appears to account for most of the difference between ΔG_{ab}^{*}(obsd) and ΔG_{ab}^{*}(OS,calcd) for the $Co^{II}(N_4)$ reductants.[5c,d]

The polypyridyl–copper(I) complexes may function principally as simple electron-transfer agents toward coordinated superoxide. For example, no reactions were observed for $Cu(bpy)_2^{+}$ even though the outer-sphere rate of electron transfer to the O_2^{-} moiety would have been only a little smaller than the rate limit dictated by the usable range of reagent concentrations. The apparent unimportance of the inner-sphere, or adduct formation, pathway for Cu^{I}(polypyridyl) complexes stands in marked contrast to the behavior of $Cu(C_2H_4)^{+}$ and $CuCl_3^{2-}$. A very small apparent rate advantage of the adduct formation pathway for the $Co([14]aneN_4)(OH_2)O_2^{2+}$–$Cu^{I}$(polypyridyl) reactions might originate from (a) a small inner-sphere reorganizational barrier to electron transfer in these systems (as manifested in the relatively large inferred self-exchange rates) so that there is no kinetic advantage to barrier reduction through adduct formation, (b) the possibility that the stability of the Cu^{II}–(O_2^{2-}) bond is not great enough to decrease by a significant amount the intrinsic barrier to electron transfer, and/or (c) relatively slow substitution into the Cu(polypyridyl) coordination sphere.

Conclusions

The observations reported in this study strongly suggest that the discrimination between the outer-sphere electron-transfer and the adduct formation pathways for the reactions of simple Cu(I) complexes with coordinated dioxygen is largely kinetic in origin and can be correlated with the size of the intrinsic reorganizational barriers to electron transfer. This variation in the discrimination between limiting reaction pathways is reminiscent of the O_2-bonding vs. electron transport functions proposed for various copper enzymes. The ability of a given copper system (complex or enzyme) to discriminate between mechanistically different reaction pathways (which are similar in the thermodynamic driving force) apparently depends on the magnitude of the first coordination sphere reorganization energy which accompanies the Cu(II)–Cu(I) electron exchange. Thus, relatively rigid coordination environments tend to result in relatively small intrinsic reorganizational barriers and favor the electron transport function. Relatively flexible coordination environments, and systems in which the Cu(II) and Cu(I) complexes have distinctly different coordination geometries, tend to have large intrinsic reorganizational barriers to simple electron transfer and to favor a concerted binding–redox process in reactions with dioxygen moieties.

Registry No. $Co([14]aneN_4)(OH_2)O_2^{2+}$, 83784-58-1; $Ru(NH_3)_4phen^{3+}$, 69799-62-8; $Co(Me_4[14]tetraeneN_4)Cl_2^{+}$, 43225-24-7; $Co(Me_6[14]\text{-}4,11\text{-}dieneN_4)(OH_2)_2^{3+}$, 17815-30-4; $Co(bpy)_3^{3+}$, 19052-39-2; $Cu(phen)_2^{+}$, 17378-82-4; $Cu(2,9\text{-}Me_2phen)_2^{2+}$, 14875-91-3; $CuCl_2^{-}$, 15697-16-2; $Cu(CH_3CN)_2^{+}$, 22418-38-8; $Cu(Im)_2^{+}$, 27858-34-0; $CuCl_3^{2-}$, 29931-61-1; $Cu(C_2H_4)(H_2O)_2^{+}$, 92366-27-3; $Cu(tpy)(H_2O)^{+}$, 92366-28-4; $Cu(bpy)_2^{+}$, 36450-97-2; $Cu(4,4'\text{-}Me_2bpy)_2^{+}$, 92366-29-5.

Supplementary Material Available: Tables of kinetic parameters (12 pages). Ordering information is given on any current masthead page.

Contribution from the Department of Chemistry,
University of New Brunswick, Fredericton, New Brunswick, Canada E3B 6E2

Solvent Effects on Redox Reactions. 1. Chromium(II) Reduction of Tris(pentane-2,4-dionato)cobalt(III) in Water/Dimethylformamide Solvent Mixtures

NITA A. LEWIS* and ANANDA M. RAY

Received August 15, 1983

The Cr(II) reduction of $Co(ptdn)_3$ was studied in various dimethylformamide/water mixtures at μ = 1.00 M (CH_3COOLi). The activation parameters were measured over a temperature range of 25–45 °C. Three pathways for reduction were observed—outer sphere, monobridged inner sphere, and dibridged inner sphere. Only the dibridged pathway showed an acid dependence. The outer-sphere and monobridged inner-sphere routes followed simple second-order kinetics whereas the dibridged path showed evidence for the presence of a binuclear intermediate. It was postulated that the dibridged transition state was stabilized by an organic solvent cage.

Introduction

Except for isotopic exchange reactions,[1-3] there have been few attempts to study the effect of solvent on electron-transfer reactions. The most comprehensive series of experiments was performed by Watts and co-workers.[4-9] This group studied the Fe(II) reductions of a series of $Co(NH_3)_5X^{2+}$ complexes where X = F^-, Cl^-, Br^-, and N_3^-, in dimethyl sulfoxide, dimethyl sulfoxide/water mixtures, and *N*,*N*-dimethylformamide. The reactions were investigated over a range of temperatures, ionic strengths, and acidities. Because of the lability of the Fe(III) products formed, the product criterion for establishing the mechanism of reduction (inner or outer sphere) could not be used. Watts and his co-workers interpreted their results in terms of an inner-sphere process in all cases using indirect methods.

A reductant that is capable of distinguishing between an inner- and an outer-sphere mechanism is Cr(II). When this reductant is used, the bridging ligand is captured in the first coordination sphere of the Cr(III) product if an inner-sphere pathway is operating, and the product is usually sufficiently robust that it can be purified by ion-exchange techniques and identified spectroscopically. In spite of the obvious advantages of using this reductant to establish the mechanism of electron transfer, few solvent studies have employed Cr(II) as a re-

(1) Sutin, N. *Ann. Rev. Phys. Chem.* **1966**, *17*, 119.
(2) Taube, H. *Advan. Inorg. Chem. Radiochem.* **1959**, *1*, 1.
(3) Halpern, J. *Q. Rev., Chem. Soc.* **1961**, *15*, 207.
(4) Matthews, B. A.; Watts, D. W. *Inorg. Chim. Acta* **1974**, *11*, 127.
(5) Matthews, B. A.; Watts, D. W. *Aust. J. Chem.* **1976**, *29*, 97.
(6) Matthews, B. A.; Turner, J. V.; Watts, D. W. *Aust. J. Chem.* **1976**, *29*, 551.
(7) Beckham, K. R.; Watts, D. W. *Aust. J. Chem.* **1979**, *32*, 1425.
(8) Westcott, T. J.; Watts, D. W. *Aust. J. Chem.* **1979**, *32*, 2139.
(9) Spiccia, L.; Watts, D. W. *Aust. J. Chem.* **1979**, *32*, 2275.

0020-1669/84/1323-3698$01.50/0

ducing agent. Nevertheless, one interesting experiment was reported in which $Cr(ptdn)_2$ where ptdn = pentane-2,4-dione was used to reduce (tetraphenylporphine)iron(II) in benzene.[10,11]

The model reaction we have chosen to investigate the effect of solvent on different redox mechanisms is the Cr^{2+} reduction of $Co(ptdn)_3$. This reaction is uniquely suited for a study of this sort since, at least in water,[12] it proceeds simultaneously by inner-sphere and outer-sphere pathways. Because Cr(III) is substitution inert, the products of reduction allow an unambiguous assignment of mechanism. We present in this work a detailed study of the addition of dimethylformamide to our model redox process. In this case, the effect on both inner-sphere and outer-sphere mechanisms is simultaneously determined under identical reaction conditions, making comparisons easy and meaningful. Activation parameters were measured since, if $\Delta H^{\ddagger}$ and $\Delta S^{\ddagger}$ were markedly dependent on the solvent present and if we had a detailed understanding of how and why this happens, redox reactions could potentially be controlled in a predictable manner by using the proper mix of solvents. If, for example, inner-sphere and outer-sphere processes are affected in opposite ways by the addition of a given solvent, this technique may eventually by used to inhibit unwanted side reactions or to accelerate desired processes in a useful system based on transition-metal redox catalysts.

Experimental Section

Reagents. Tris(pentane-2,4-dionato)cobalt(III), $Co(ptdn)_3$, was obtained from ICN Pharmaceuticals Inc. and was used as received. All reagent solutions were prepared in water, which was deionized with a Barnstead high-capacity ion exchanger, and then distilled with a Barnstead Fi-stream glass distillation apparatus and finally redistilled from alkaline permanganate in an all-glass apparatus. Spectroscopic grade dimethylformamide (DMF) was obtained from Alfa Products and was used without further purification.

The lithium salt of trifluoroacetic acid was prepared by dissolving the stoichiometric amount of lithium carbonate (54.0 g, G. Frederick Smith Chemical Co.) in trifluoroacetic acid (168 g, Aldrich Chemical Co. Inc.) diluted with 200 mL of purified water. This solution was then evaporated to dryness, and the resulting salt was dissolved in dimethylformamide. Triplicate portions of this stock solution (~2.7 M) were then standardized by determining titrimetrically the amount of hydrogen ion released from an Amberlite IR-120(H) analytical grade resin (BDH Chemicals Ltd.).

A standard solution of trifluoroacetic acid in DMF (~3.0 M) was prepared. An aliquot of this solution was diluted 25 times with water, and the hydrogen ion concentration was determined titrimetrically. A blank was also prepared by titrating a known amount of trifluoroacetic acid in the presence of the same quantity of DMF as was contained in the unknown. An aqueous solution of trifluoroacetic acid (~2.8 M) was prepared and analyzed titrimetrically, as well.

Chromium(II) stock solutions were made from chromium pellets (99.99% pure, Ultrex grade, J. T. Baker Chemical Co.). The metal pellets were then scratched by using an electric engraver and were activated by placing the scratched pellets in 3 M HCl. As soon as all pellets had started to react, they were removed from the acid solution, washed several times with water, and dried. The chromium pellets were then placed into a deaerated solution of standard ~1.0 M trifluoroacetic acid and were allowed to dissolve completely. The concentration of Cr(II) in the final solution was determined every 3 days by a standardization procedure described earlier.[13]

All standard solutions were stored under high-purity argon and were handled by using standard syringe techniques in an argon atmosphere.

Kinetic Measurements. The rate of reduction of $Co(ptdn)_3$ by Cr(II) was followed using a stopped-flow spectrophotometer (Dionex Model D-110) interfaced to an Explorer II digital oscilloscope (Nicolet Instrument Corp.). The water bath on the stopped-flow instrument was connected to a Lauda NB-D temperature-controlled bath having an R2U Electronic Universal Relay unit. The temperature was controlled with a mercury-contact thermoregulator and was monitored in the water bath of the stopped-flow instrument using an ASTM thermometer calibrated from 0 to 50 °C (Fisher Scientific).

All reactions were carried out under pseudo-first-order conditions; i.e., the reductant was always present in greater than 20-fold excess over the oxidant. The ionic strength in each experiment was controlled to 1.00 with the standard lithium trifluoroacetate solution.

Product Analyses. In the first series of experiments, approximately equal proportions of $Co(ptdn)_3$ (140 μ mol) and Cr(II) (145 μmol) were mixed together in 20 mL of the desired solvent mixture. The proportion of DMF in the aqueous medium varied from 0% to 90% by volume, and the analyses were performed at 25, 35, and 45 °C. In all cases, the acid concentration was controlled to 0.10 M by using the standard stock CF_3COOH solutions. The reaction was allowed to continue to completion. Some reaction mixtures were allowed to proceed for 5 half-times and others for 10 half-times. The reaction mixture was then diluted to 500 mL with cold distilled water. Air was bubbled through the solution for about 5 min, and a cation-exchange column (Dowex 50W-X8(200)) was charged with this aerated solution. The excess of dimethylformamide was washed from the column with distilled water. Following this, the three products were separated into distinct bands by eluting with a solution of 6.25×10^{-2} M $NaClO_4$ in 1.25×10^{-2} M $HClO_4$. The first band, identified as $Cr(solv)_2(ptdn)_2^+$ where solv is water or DMF, was eluted with 6.25×10^{-2} M $NaClO_4$ in 1.25×10^{-2} M $HClO_4$. The second band, $Cr(solv)_4(ptdn)^{2+}$ was removed from the column by elution with 0.50 M $NaClO_4$ in 0.10 M $HClO_4$. The final compound, $Cr(solv)_6^{3+}$, came off the column by elution with a mixture of 1.0 M $NaClO_4$ in 0.2 M $HClO_4$. The chromate content of each band was estimated using a standard chromate analysis.[14]

In the second series of product studies, the acid dependence of the reaction was investigated at 25.0 °C in all solvent mixtures.

Spectral Measurements. All electronic spectra of reaction products and chromium(III)-solvated species were obtained on a Perkin-Elmer Model 330 UV–vis–near-IR spectrophotometer.

Results

The rates of reduction of $Co(ptdn)_3$ by Cr(II) (at 0.10 M $[H^+]$ and μ = 1.00) were measured in various dimethylformamide/water mixtures. The overall rate constants are listed in Table I; these were decomposed into three pathways—monobridged inner sphere, dibridged inner sphere, and outer sphere—using the product analysis results of Table II. The component rate constants derived in this fashion are collected in Table I; their dependence as a function of the mole fraction of DMF present in the reaction medium at 25 °C is shown graphically in Figure 1. The rate constants for the outer-sphere and monobridged inner-sphere paths increase to a maximum at about 0.3 mole fraction DMF (abbreviated χ_{DMF}) whereas the dibridged path increases with increasing DMF in the reaction medium until χ_{DMF} = 0.5. Then, the rate constant begins to decrease as the DMF concentration is further increased.

Activation parameters derived for each of the three pathways are collected in Table III. The changes that occur in $\Delta H^{\ddagger}$ and $\Delta S^{\ddagger}$ as the mole fraction of DMF in the medium increases, for each pathway, are presented graphically in Figures 2 and 3, respectively. In both cases, for the monobridged pathway, an extreme is reached at about χ_{DMF} = 0.15 and 0.3. The dibridged pathway shows the most extreme behavior at χ_{DMF} = 0.5, although the graph shows a local minimum for $\Delta H^{\ddagger}$ and $\Delta S^{\ddagger}$ at χ = 0.15. The outer-sphere pathway is least strongly influenced by the presence of dimethylformamide; a weak maximum appears at χ_{DMF} = 0.15 for $\Delta H^{\ddagger}$ and at χ_{DMF} = 0.5 for $\Delta S^{\ddagger}$.

The acid dependencies of the three pathways were measured at 25 °C, and the results obtained are presented in Tables IV and V. For the monobridged and outer-sphere pathways, there was no effect on the rate that could be ascribed to the acidity of the medium. However, the k_{obsd} for the dibridged

(10) Cohen, I. A.; Jung, C.; Governo, T. *J. Am. Chem. Soc.* **1972**, *94*, 3003.
(11) A brief qualitative study in methanol/water mixtures has also appeared: Thomas, J. C.; Reed, J. W.; Gould, E. S. *Inorg. Chem.* **1975**, *14*, 1696.
(12) Linck, R. G.; Sullivan, J. C. *Inorg. Chem.* **1967**, *6*, 171.
(13) Balahura, R. J.; Jordan, R. B. *J. Am. Chem. Soc.* **1970**, *92*, 1533.
(14) Balahura, R. J.; Jordan, R. B. *J. Am. Chem. Soc.* **1973**, *95*, 1137.

Table I. Kinetic Data for the Cr(II) Reduction of $Co(ptdn)_3$ in Dimethylformamide/Water Mixtures at $[H^+] = 0.10$ M and $\mu = 1.00$ M (CF_3COOLi)[a]

mole fraction DMF	temp,[a] °C	$10^4 \times [Co(ptdn)_3]$[b]	$10^2 \times [Cr(II)]$[b]	$k_{overall}$, $M^{-1}\ s^{-1}$	k_{mono},[c] $M^{-1}\ s^{-1}$	k_{di},[d] $M^{-1}\ s^{-1}$	k_{outer},[e] $M^{-1}\ s^{-1}$
0.00	25.0	6.96	2.77	8.81	4.04	0.352	4.39
	35.0	6.96	2.77	15.0	8.07	0.811	6.15
	45.0	6.96	2.77	24.1	14.5	1.59	7.98
0.025	25.0	7.05	2.84	24.6	4.3	0.63	8.5
0.055	25.0	6.99	6.12[f,j]	24.4	7.81	1.15	15.4
0.134	25.0	7.04	4.79[g,j]	45.7	13.2	2.49	29.9
	35.0	7.01	2.79	62.3	19.6	4.54	38.1
	45.0	7.01	2.79	94.0	33.6	8.92	51.3
0.259	25.0	7.01	4.50[h,j]	59.0	16.0	4.22	38.8
	35.0	7.01	2.79	90.3	24.4	9.03	56.9
	45.0	7.01	2.79	143	51.4	18.3	73.1
0.481	25.0	7.03	3.18[i,j]	53.1	14.8	7.96	30.2
	35.0	7.05	2.86	81.7	24.5	18.8	38.4
	45.0	7.05	2.86	153	44.3	44.3	64.2
0.568	25.0	7.05	2.86	45.7	11.1	9.4	25.2
0.676	25.0	7.03	2.81	39.0	8.92	8.40	21.7
	35.0	7.01	2.77	57.1	16.9	12.8	27.4
	45.0	7.01	2.77	92.7	27.8	23.8	41.1

[a] The temperature was controlled to ±0.1 °C or better. [b] All concentrations are initial values given in molar units. [c] This is the rate of reaction proceeding through the monobridged pathway and is obtained by multiplying the overall rate with the average fraction of the monobridged product produced. [d] This is the rate of reaction proceeding through the dibridged pathway and is obtained by multiplying the overall rate with the average fraction of the dibridged product produced. [e] This is the rate of reaction proceeding through outer-sphere pathway and is obtained by taking the difference between the overall rate and the total rate for the inner-sphere pathways. [f] Average of concentrations ranging from 2.84×10^{-2} to 1.41×10^{-1} M. [g] Average of concentrations ranging from 1.41×10^{-2} to 1.41×10^{-1} M. [h] Average of concentrations ranging from 1.27×10^{-2} to 12.8×10^{-1} M. [i] Average of concentrations ranging from 1.43×10^{-2} to 5.65×10^{-2} M. [j] There was no dependence of the second-order rate constant, $k_{overall}$, on the concentration of Cr(II).

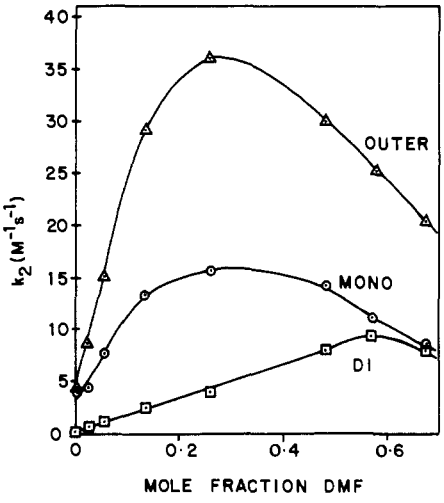

Figure 1. Rate dependence of each pathway on mole fraction of dimethylformamide in the reaction mixture at $[H^+] = 0.10$ and $\mu = 1.00$ (CF_3COOLi).

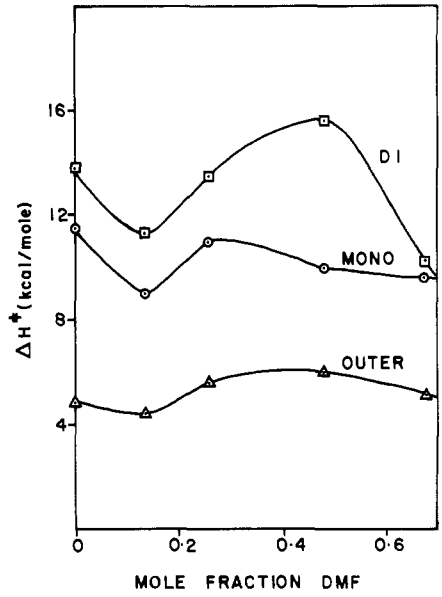

Figure 2. Dependence of $\Delta H^{\ddagger}$ for each pathway on mole fraction of dimethylformamide.

inner-sphere path contained a term inverse in hydrogen ion concentration. This effect was observed at all dimethylformamide/water mixtures studied.

From these results, the rate law for the monobridged and outer-sphere pathways at a particular dimethylformamide/water ratio is in both cases

$$-\frac{d[Co(ptdn)_3]}{dt} = k_2[Co(ptdn)_3][Cr(II)] \quad (1)$$

whereas the rate law for the dibridged pathway is of the form

$$-\frac{d[Co(ptdn)_3]}{dt} = \left[a + \frac{b}{[H^+]}\right][Co(ptdn)_3][Cr(II)] \quad (2)$$

Numerous attempts were made to determine the ratio of DMF to water ligands in the final products. All of these failed due to the lability of at least one of the DMF ligands in the products. The UV–vis spectra of the $Cr(solv)_2(ptdn)_2^+$ and $Cr(solv)_4(ptdn)^{2+}$ species from each column were variable but similar. If the solutions containing these complexes were diluted and passed through a second ion-exchange column, the charge was unchanged, indicating that the chelated ptdn ligands survived intact but the UV–vis spectra taken before and after the second ion-exchange procedure were slightly different and again variable presumably due to replacement of DMF ligands by water. Allowing the solutions to sit for 1 week at room temperature did not result in generation of spectra that matched completely those of the known fully aquated species, although loss of the pentane-2,4-dione ligand was negligible. This indicates that at least some of the DMF ligands are fairly inert.

Discussion

The most surprising outcome of this investigation was the observation of the dibridged inner-sphere mechanism. The reduction of $Co(ptdn)_3$ by Cr(II) in aqueous solution was

Table II. Product Analysis Data for the Cr(II) Reduction of $Co(ptdn)_3$ in Dimethylformamide/Water Mixtures at $[H^+] = 0.10$ M[a]

mole fraction DMF	temp,[b] °C	Cr(II) μmol used	$Co(ptdn)_3$ μmol used	$Cr(OH_2)_4(ptdn)^{2+}$ μmol recovered	$Cr(OH_2)_2(ptdn)_2^+$ μmol recovered	% mono path[c]	% di path[d]
0.00	25.0	146	140	64.4	5.52	46.0	3.95
	35.0	146	140	75.1	7.49	53.7	5.35
	45.0	146	140	84.4	9.18	60.3	6.55
0.055	25.0	146	141	44.7	6.70	31.8	4.75
0.134	25.0	146	141	40.3	7.77	28.6	5.52
	35.0	147	140	44.3	10.3	31.5	7.33
	45.0	147	140	50.2	13.4	35.8	9.57
0.259	25.0	147	141	38.1	10.1	27.1	7.18
	35.0	147	141	38.7	14.1	27.5	10.0
	45.0	147	141	51.3	17.9	36.5	12.8
0.481	25.0	145	141	39.0	21.0	27.7	14.9
	35.0	145	141	43.0	32.4	30.5	22.9
	45.0	145	141	40.6	40.8	28.8	29.0
0.568	25.0	146	141	34.3	28.9	24.3	20.5
0.676	25.0	145	141	32.3	30.3	22.9	21.5
	35.0	146	141	41.6	31.8	29.5	22.6
	45.0	146	141	42.6	36.2	30.2	25.7

[a] Quoted values are all averages of two to five (usually three) runs per point. [b] The temperature was accurate to within ±0.10 °C. [c] This is the percentage of the reaction that proceeded by the monobridged transition state based on mol of $Cr(H_2O)_4(ptdn)^{2+}$ recovered/mol of $Co(en)(ptdn)_2^+$ used. [d] This is the percentage of the reaction that proceeded by the dibridged transition state based on mol of $Cr(H_2O)_2(ptdn)_2^+$ recovered/mol of $Co(en)(ptdn)_2^+$ used.

Table III. Summary of Rate Constants and Activation Parameters[a] for the Cr(II) Reduction of $Co(ptdn)_3$ at $[H^+] = 0.10$ M and $\mu = 1.00$ M (CF_3COOLi)

mole fraction DMF	path-ways	k(25 °C), M^{-1} s^{-1}	$\Delta H^{\ddagger}$, kcal/mol	$\Delta S^{\ddagger}$, eu
0.000	mono	4.11 ± 0.04	11.4 ± 0.6	−18 ± 2
	di	0.352 ± 0.007	14 ± 1	−15 ± 4
	outer	4.41 ± 0.06	5.0 ± 0.9	−39 ± 3
0.134	mono	12.2 ± 0.1	9 ± 1	−24 ± 3
	di	2.51 ± 0.04	11 ± 1	−19 ± 4
	outer	30.2 ± 0.3	4.3 ± 0.9	−37 ± 3
0.259	mono	15.7 ± 0.3	11 ± 1	−18 ± 4
	di	4.26 ± 0.05	13.1 ± 0.8	−12 ± 3
	outer	38.9 ± 0.5	5.3 ± 0.9	−34 ± 3
0.481	mono	14.4 ± 0.1	9.6 ± 0.5	−21 ± 2
	di	8.2 ± 0.1	16 ± 1	−2 ± 4
	outer	28.9 ± 0.8	7 ± 2	−21 ± 7
0.676	mono	9.1 ± 0.1	10.1 ± 0.8	−20 ± 3
	di	8.1 ± 0.2	9 ± 1	−23 ± 4
	outer	21.0 ± 0.4	5 ± 1	−34 ± 4

[a] The activation parameters and rate constants were calculated on an IBM 3032 computer using a least-squares program. The errors reported are standard deviations. All rate constants were multiplied by each appropriate product analysis to obtain these results. These values will therefore vary from those derived from the data in Tables I and II, which are average values. The numbers listed in this table may be obtained by using the full set of experimental values available as supplementary material.

reported in 1967 by Linck and Sullivan,[12] and only the monobridged and outer-sphere pathways were observed in aqueous solution.

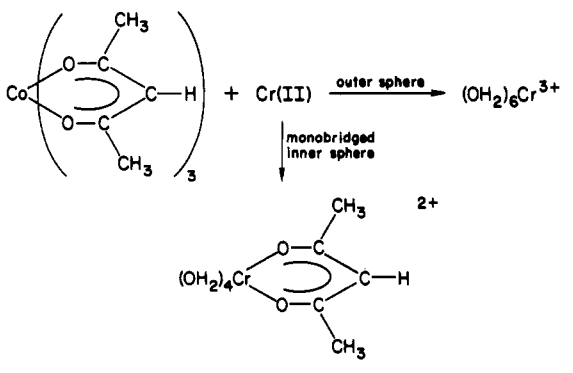

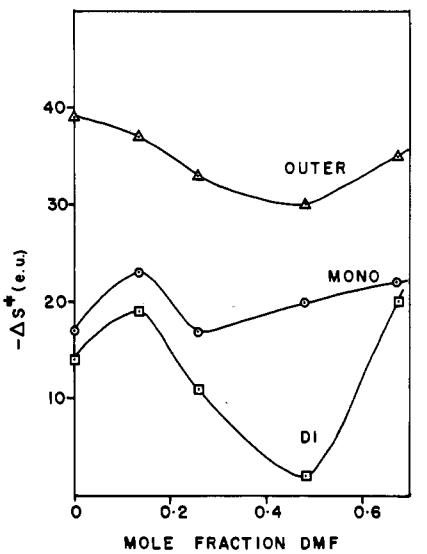

Figure 3. Dependence of $\Delta S^{\ddagger}$ for each pathway on mole fraction of dimethylformamide.

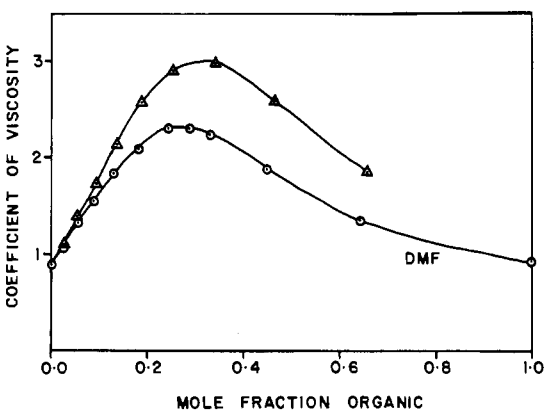

Figure 4. Dependence of coefficient of viscosity on mole fraction of organic substance in aqueous solution: O, mole fraction of DMF in water; Δ, sum of mole fractions of equal volumes of dimethylformamide and dimethyl sulfoxide in water. Values were taken from ref 15.

This was considered unusual by Balahura and Lewis,[15] who found that the Cr(II) reduction of a very similar complex,

Table IV. Kinetic Data for the Cr(II) Reduction of $Co(ptdn)_3$ in Dimethylformamide/Water Mixtures at Various Acidities at 25.0 °C and $\mu = 1.00$ M (CF_3COOLi)

mole fraction DMF	$[H^+]$, M	$10^4 \times [Co(ptdn)_3]$, M	$10^2 \times [Cr(II)]$, M	$k_{2,overall}$, $M^{-1}\ s^{-1}$	k_{mono},[a] $M^{-1}\ s^{-1}$	k_{di},[b] $M^{-1}\ s^{-1}$	k_{outer},[c] $M^{-1}\ s^{-1}$
0.055	0.10	var	var	24	7.7	1.13	15
	0.20	7.01	2.81	23.5	7.68	0.675	15.2
	0.40	7.01	2.81	21.7	7.99	0.614	13.1
	0.60	7.01	2.81	19.2	6.14	0.346	12.7
	0.80	7.01	2.81	18.3	6.24	0.315	11.7
0.134	0.10	var	var	46	13	2.4	28
	0.40	6.96	2.83	44.1	13.7	1.76	28.6
	0.50	6.96	2.83	38.3	12.9	1.31	24.1
	0.60	6.96	2.83	38.9	12.6	1.05	25.3
	0.80	6.96	2.83	38.3	12.5	0.904	24.9
0.189	0.05	7.03	2.82	55.2	16.0	4.07	35.1
	0.10	7.03	2.82	55.9	14.2	3.23	38.5
	0.20	7.03	0.85	52.6	14.7	2.86	35.0
	0.50	7.03	2.82	52.3	16.2	1.83	34.3
0.481	0.10	7.03	var	53	15	8	30
	0.20	7.06	2.83	56.3	17.2	6.98	32.1
	0.40	7.06	2.83	56.3	18.8	6.02	31.5
	0.80	7.06	2.83	54.4	17.8	4.45	34.1
	0.80	7.01	2.80	54.8	17.9	4.33	32.6
0.676	0.10	var	var	39	8.9	8.4	22
	0.20	7.06	2.83	36.8	11.6	6.15	19.1
	0.40	7.06	2.83	41.5	12.1	5.52	19.8
	0.80	7.06	2.83	38.9	11.9	3.93	23.1

[a] These are the rate constants for monobridged pathway and are obtained by multiplying the overall rate with the fraction of monobridged inner-sphere product produced in the reaction mixture with the same solvent composition. [b] Rate constants for the dibridged pathway are obtained by multiplying the overall rate with the fraction of dibridged products produced in the reaction mixture with the same solvent composition. [c] These are the rate constants for the outer-sphere pathways and are obtained by taking the difference between the overall rate constants and the rate constants for the total inner-sphere pathways.

bis(pentane-2,4-dionato)(ethylenediamine)cobalt(III) proceeded partly by a dibridged inner-sphere pathway as well as by the monobridged inner-sphere and outer-sphere routes.

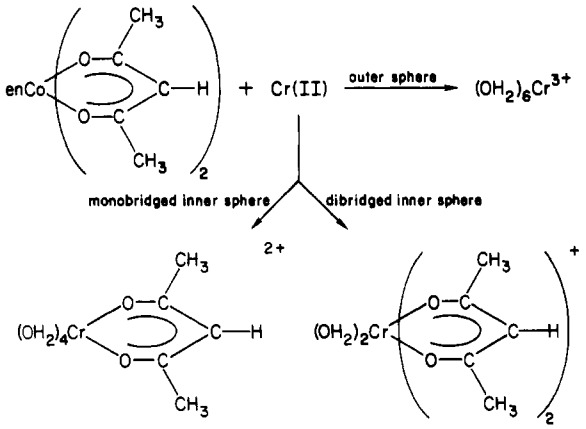

At that time, the factors leading to double bridging were neither well understood nor predictable. In the present work, we discovered that solvent effects play a predominant role in stabilizing the transition state for dibridged transfer.

The point of maximum viscosity in the solvent mixture ($\chi_{DMF} = 0.3$, see Figure 4), corresponds to the maximum rate of electron transfer by either the monobridged inner-sphere or outer-sphere mechanisms ($\chi_{DMF} = 0.3$, see Figure 1). This implies a difference in the way the solvent molecules pack together at higher DMF concentrations, probably beginning to form "organic clusters" at this point. If these clusters begin to preferentially solvate the metal complexes, it may be difficult for the two redox partners to approach each other at sufficiently close distances that the electron-transfer reaction could occur. In other words, the outer-sphere reorganization energy, $\Delta G_0^{\ddagger}$, appears to be greatly affected by the presence of DMF in the medium, perhaps because of the difficulty of organizing solvent clusters after a mole fraction of 0.3 DMF is reached, as opposed to fairly discrete DMF and water molecules in the case of media having low organic content.

The situation for dibridged transfer is somewhat different. The rate of electron transfer by the dibridged transition state continues to increase beyond the point of maximum viscosity. In fact, from Figure 1, it can be seen that the rate constant for electron transfer, using this route, increases until the mole fraction of DMF reaches about 0.5; then, it begins to decrease slowly. It appears that the DMF solvent cage is crucial to the stabilization of the dibridged transition state, since this pathway was not employed to a very significant extent in a purely aqueous medium. Probably, the organic solvent cage keeps the oxidant and reductant in contact long enough for two bonds to form between them prior to the act of electron transfer.

The most extreme behavior in terms of the activation parameters is exhibited by the dibridged pathway. The enthalpic barrier for electron transfer via this path reaches a maximum when $\chi_{DMF} = 0.5$. The huge contribution of the entropy of activation to the overall free energy for this process (see Figure 3) is responsible for the rather facile rate observed for the dibridged route in this solvent composition. It appears that the reacting pairs are caught in large solvent cages that make escape difficult. The large enthalpic barrier is probably due to the rearrangement of the solvent surrounding each metal ion so that the two reacting species may approach each other.

Watts and his co-workers[4-9] have studied the Fe(II) reductions of a series of complexes $Co(NH_3)_5X^{2+}$ where X = F^-, Cl^-, Br^-, and N_3^- in Me_2SO and Me_2SO/H_2O solvent mixtures. They also observed dramatic rate changes at $\chi_{Me_2SO} = 0.3$ and suggested that this corresponded to the preferential solvation of the Fe(II) by Me_2SO, which became complete at $\chi_{Me_2SO} = 0.3$. They postulated that further substitution of Me_2SO for H_2O in the coordination sphere of iron(II) in both the chloro and bromo systems leads to a stabilization of the

(15) Balahura, R. J.; Lewis, N. A. *J. Am. Chem. Soc.* **1977**, *99*, 4716.
(16) Jannakoudakis, D.; Papanastasiou, G.; Mavridis, P. G. *Chem. Chron.* **1976**, *5*, 167; *Chem. Abstr.* **1977**, *86*, 8849*IV*.
(17) Balahura, R. J.; Lewis, N. A. *J. Chem. Soc., Chem. Commun.* **1976**, 268.

Table V. Product Analysis Data for the Cr(II) Reduction of $Co(ptdn)_3$ in Dimethylformamide/Water Mixtures at Various Acidities and 25.0 °C

mole fraction DMF	$[H^+]$, M	Cr(II) μmol used	$Co(ptdn)_3$ μmol used	$Cr(OH_2)_4(ptdn)^{2+}$ μmol recovered	$Cr(OH_2)_2(ptdn)_2^+$ μmol recovered	% mono path[a]	% di path[b]
0.055	0.10	var	141	var	var	32	4.7
	0.20	145	143	46.5	4.10	32.7	2.87
	0.40	145	142	52.3	4.03	36.8	2.83
	0.60	145	142	45.5	2.56	32.1	1.80
	0.80	145	141	48.0	2.43	34.1	1.72
0.134	0.10	var	var	var	var	29	5.5
	0.40	142	141	43.6	5.60	31.1	4.00
	0.60	145	144	46.8	3.90	32.5	2.69
	0.80	142	141	45.7	3.30	32.6	2.36
0.189	0.05	145	142	41.0	10.4	29.0	7.38
	0.10	145	143	36.1	8.22	25.4	5.77
	0.20	145	141	39.4	7.70	27.9	5.44
	0.50	145	141	44.2	5.01	30.9	3.50
0.481	0.10	145	141	var	var	28	15
	0.20	142	141	43.2	17.5	30.6	12.4
	0.20	145	143	40.4	15.4	28.9	11.0
	0.40	146	143	47.8	15.3	33.4	10.7
	0.40	145	140	40.1	14.7	28.0	10.3
	0.80	142	141	44.9	11.0	32.7	7.90
0.676	0.10	var	141	var	var	22.9	21.5
	0.20	145	141	44.4	23.6	31.5	16.7
	0.40	145	142	41.5	18.9	29.2	13.3
	0.80	145	139	42.4	14.1	30.5	10.1

[a] This is the percentage of the reaction that proceeded by the monobridged transition state based on mol of $Cr(H_2O)_4(ptdn)^{2+}$ recovered/mol of $Co(en)(ptdn)_2^+$ used. [b] This is the percentage of the reaction that proceeded by the dibridged transition state based on mol of $Cr(H_2O)_2(ptdn)_2^+$ recovered/mol of $Co(en)(ptdn)_2^+$ used.

tetrahedral intermediate whereas, for inner-sphere attack at the fluoro ligand, since the coordination sphere about the iron(II) remains octahedral, the rate does not change as more Me_2SO is added to the medium. This interpretation was challenged by van Eldik et al.,[18] who concluded on the basis of ΔV^* measurements on the same system that the results were best interpreted due to changes in solvation and the introduction of steric crowding rather than by changes in the coordination number of Fe(II).

The possibility of significant concentration of four-coordinate chromium(II) species being present in the bulk solvent in our studies seem to be excluded by the visible spectra of this extremely labile metal ion in the DMF/water mixtures used in the present study (see Figure 5). Four-coordinate Cr(II) would be expected to have a visible spectrum very different from that of the corresponding octahedral species, but in fact no significant change was noted in the absorption maxima of the spectra as the proportion of DMF in the medium was increased. The only effect noted was a gradual increase in extinction coefficient with increasing organic content in the bulk solvent. From the kinetic studies of van Eldik et al.,[18] it was similarly concluded that the replacement of coordinated water molecules on Fe(II) is a gradual process. Unless these reductions are significantly nonadiabatic in character, there does not seem to be any evidence supporting the concept of four-coordinate Fe(II) or Cr(II) in the transition state.

We note that the viscosity of the medium reaches a maximum at $\chi = 0.3$ both for DMF/water mixtures and for DMF/Me_2SO/water mixtures if one plots mole fraction of total organic against viscosity (Figure 4).[16] Since reaction rates tend to peak at this value so consistently for completely unrelated systems, we propose that this phenomenon may be due to contributions of ΔG_0^* arising from clustering in the bulk solvent, which begins to appear at this point.

Our experiments also served to dispel the notion[8] that inner-sphere reactions could be accelerated to a greater extent than outer-sphere processes in the presence of an organic solvent. Figure 1 shows, in fact, that the outer-sphere reaction initially experiences a greater acceleration than the inner-sphere pathways *for the same complex studied at the same time under identical conditions.*

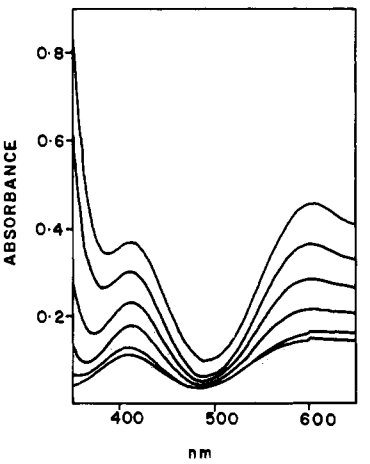

Figure 5. Absorbance of chromium(II) in various dimethylformamide/water mixtures. Mole fractions of DMF from lowest spectrum to highest one: 0.000, 0.055, 0.134, 0.259, 0.481 and 0.676. Concentrations (M): $[Cr(II)] = 4.32 \times 10^{-3}$, $[H^+] = 0.10$ (CF_3COOH) in all spectra.

The outer-sphere and monobridged inner-sphere pathways show simple second-order kinetics with no acid dependencies (Table IV). The observed rate constant for the dibridged path did, however, contain a term inverse in acid concentration since a linear relationship was obtained by plotting $1/k_{D1}$ vs. $[H^+]$. This implies that the cobalt complex exists in both protonated and unprotonated forms, with the unprotonated forms being more reactive. The observed rate constant derived from this mechanism is

$$k_{D1} = (k_1[H^+] + k_2K_a)/(K_a + [H^+])$$

(18) van Eldik, R.; Palmer, D. A.; Kelm, H. *Inorg. Chim. Acta* **1978**, *29*, 253.

Table VI. Values of k_2 and K_a for the Dibridged Pathway Calculated from the Slopes and Intercepts of Plots of $1/k_{D1}$ vs. $[H^+]$

mole fraction DMF	slope	intercept	k_2 (eq 33)	K_a	standard error
0.055	3.3	0.6	1.6	0.2	0.3
0.134	1.04	0.26	3.9	0.25	0.08
0.189	0.64	0.23	4.4	0.36	0.02
0.481	0.15	0.11	9.1	0.73	0.003
0.676	0.18	0.11	9.1	0.61	0.01

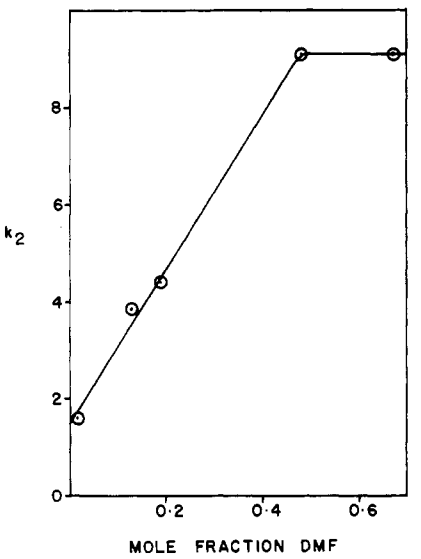

Figure 6. Dependence of k_1 on mole fraction DMF for the dibridged pathway.

Assuming that k_1 is very small, then the expression reduces to

$$k_{D1} = k_2 + k_2K_a/[H^+]$$

which is consistent with the empirical rate expression given in eq 2.

A plot of $1/k_{D1}$ vs. $[H^+]$ gives a straight line having an intercept of $1/k_2$ and a slope of $1/k_2K_a$. Table VI lists the values of k_2 and K_a calculated from these plots. The pK_a values ranging from 0.21 to 0.72 calculated from these data indicate that $Co(ptdn)_3$ is a strong acid in the media studied.

The form of the binuclear intermediate must be such that two bridges are formed with Cr(II) prior to electron transfer as was postulated earlier in the reduction of the $Co(en)(ptdn)_2^+$ complex.[15,17] A possible form of the intermediate is shown in which arbitrarily only one of the pentane-2,4-dione rings is shown protonated.

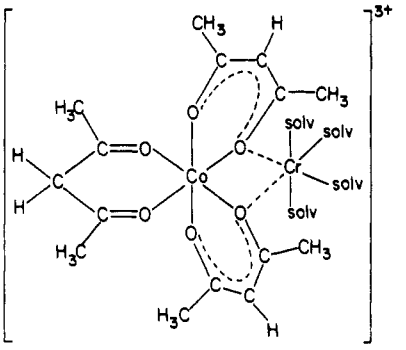

The rate of reaction is most sensitive to expulsion of this proton for solvents having low mole fractions of dimethylformamide (see Figure 6).

Our experiments have delineated some of the effects that are important to the stabilization of the dibridged transition state. The formation of a long-lived solvent cage seems to be most crucial to the observation of this pathway. The dibridged mechanism, at least for the Cr(II) reduction of $Co(ptdn)_3$, is sensitive to the presence of acid and displays a term inverse in hydrogen ion concentration. Whether this is due to the reduced charge in the transition state favoring the approach of the metal species or to changes in the electronic nature of the chelated pentane-2,4-dionato ligand as it becomes protonated cannot be determined from our studies. We are presently studying this model reaction in a variety of different solvent mixtures in an attempt further to uncover the subtle nuances governing these basic types of redox processes.

Acknowledgment. We are very grateful to the Natural Sciences and Engineering Research Council of Canada for an operating grant and an equipment grant for the purchase of a UV–vis–near-IR spectrophotometer, which made this work possible.

Registry No. $Co(ptdn)_3$, 21679-46-9; DMF, 68-12-2; Cr, 7440-47-3.

Supplementary Material Available: Complete kinetic and product analysis data (Tables 1S and 2S, respectively) (9 pages). Ordering information is given on any current masthead page.